

## Review

---

# PHYSICOCHEMICAL CHARACTERIZATION OF COAL AND COAL REACTIVITY: A REVIEW

W.A. KNELLER

*Department of Geology, The University of Toledo,  
2801 W. Bancroft Street, Toledo, OH 43606 (U.S.A.)*

(Received 20 May 1986)

## ABSTRACT

This review is based on a search of the ACS chemical data base for the years 1977–1985 using the key words: *coal*, *thermal analysis* (TA), *differential scanning calorimetry* (DSC), *differential thermal analysis* (DTA) and *thermogravimetry* (TG). One-hundred and fifty-seven references on TA/coal were accrued by this computerized library search. Ninety-six of these references were in English; 26 in Russian; 9 in Japanese; 5 each in Bulgarian, Polish and German; 4 in Chinese; 3 in Belgian French; and 4 in other languages. A somewhat different approach to most of the review papers of the past is offered. Using the 96 English, as well as other additional references, papers were selected and condensed according to their import and impact on coal science, namely, coal characterization and coal reactivity — very important and appropriate subjects for determining coal quality. References were selected and condensed that were outstanding examples of tandem systems — the coupling of other methods with conventional TA methods. These other techniques include mass spectroscopy (MS), gas chromatography (GC), and infrared spectroscopy (IR).

## INTRODUCTION

There is an increasing worldwide demand for more energy, and since the energy crisis of 1973 the American public has become aware that our present energy resources are not limitless. Although there are some discrepancies as to the nature and extent of past and future fuel shortages, there is little doubt that there will be significant changes in the proportions of fossil fuels and how they are used.

During the 1970s the oil-producing nations of OPEC controlled about 40% of the oil marketplace. During this period of control, the western industrial nations were forced to re-evaluate and re-examine their own diverse sources of energy. These western industrial nations had developed an inordinate dependence on petroleum supplied by the OPEC nations and on occasion found that their supplies of fuel were subjected to disruption and a four or five-fold, or higher, increase in price. The industrial countries of the world were forced, therefore, to take a closer look at coal resources which

many of them had relied upon heavily for inexpensive energy during their rapid industrialization, especially with the industrialization of the third world!

Public and government response to energy crises caused by the OPEC nations was profound, and now, through conservation and reduced economic output and the oncoming stream of Alaskan and North Sea oil, there is a worldwide energy glut. It is possible that OPEC may be forced to reduce their price per barrel of oil from approximately US \$27 to between \$15 and \$20. Even if this reduction in price occurs, it will not solve the expected long-range shortfall in energy used by the world by the year 2000. Hubbert [1–5] has repeatedly declared that availability of oil and gas will decline, whereas future demand for energy will increase. As early as 1956 Hubbert [1] pointed out that petroleum and gas resources were non-renewable and far more limited than coal resources. He [5] quoted Averitt's [6] estimate that the total world resources of mineable coal range from  $4.3$  to  $7.6 \times 10^{12}$  metric tons (tonnes) with about  $1486 \times 10^9$  tonnes for the U.S. alone.

With this decline in available oil and gas the United States, as well as western Europe and Japan, will need to develop advanced energy systems. Coal as an interim or augmentation fuel could give the world the time needed to develop these advanced systems with a minimum amount of economic and political dislocation. However, some problems still remain. Over the next decade and a half (1985–2000), the United States expects to increase its use of coal with a total contribution to the total U.S. energy consumption profile of  $\sim 30$  quadrillion BTUs. To gain this energy output from coal it will be necessary that coal's share of the U.S. fuel market be increased from  $\sim 17\%$  to  $\sim 32\%$ . To meet these needs the U.S. Geological Survey has determined that the U.S. has  $\sim 1.7$  trillion tonnes of coal within 3000 ft. of the surface; however, only 200 billion tonnes of this coal is economically or technically feasible to mine. At a production rate of about 800 million tonnes per year (1980) the available 200 billion tonnes of coal in the U.S. would last about two centuries. However, if the U.S. increases its coal production rate to more than 2 billion tonnes per year then the available coal reserves would last us less than one century, assuming a constant rate of production of 2 billion tonnes per year. If, however, we increased production by 7% per year then the 200 billion tonnes of proven reserves would be exhausted in less than 50 years [7]. Using these estimates, massive conversion of coal to liquid transportation fuels, in reality, is not feasible. For example, if we build four coal liquefaction plants twice the size of the South African Sasol-Two complex, we will only satisfy about 3% of our daily (1980) oil consumption ( $\approx 440\,000$  bbls/day).

Gasification of coal, however, shows more promise than liquefaction; i.e., pyrolytic processes which produce coal gas and a clean burnable char, a possible boiler fuel, are more economically feasible. Much research has been done but still more is needed.

Coal will remain an important fuel and will increase in use regardless of the present world oil glut. The type of research needed to solve this dilemma will need to change. In the next five years research on coal quality will be of paramount importance. More effective, safe and clean uses of high-sulfur coals will also be important. The present author agrees with Rajeshwar [8], who stated that the extent to which the U.S. can use coal, as an interim fuel, is largely dependent upon the success of research into developing energy-efficient, economical, non-polluting products from coal.

It is necessary to characterize coal fully if its quality is to be ascertained. Thermal analysis (TA) plays an important role in determining the characteristics of coal because pyrolysis and combustion are fundamental to the use of coal. It is the purpose of this review to provide a survey of TA applications to the characterization of coal for industrial use.

## SCOPE OF THE REVIEW

Initially, the ACS chemical data base for 1977–1985 was employed using the key words: *coal, thermal analysis, differential scanning calorimetry, differential thermal analysis and thermogravimetry*. Only 157 references on TA/coal were accrued by this computerized library search.

Ninety-six of these references were in English; 26 in Russian; 9 in Japanese; 5 each in Bulgarian, Polish and German; 4 in Chinese; 3 in Belgian and French; and 4 in other languages. It was impossible to study and synthesize all these references in the time available to the author. It was decided to take a somewhat different approach to most of the review papers of the past. Using the 96 English, as well as additional references, it was decided to select TA papers according to their importance in characterizing coal and coal reactivity — salient and timely subjects for determining coal quality. The following is a brief outline of how coals are characterized for industrial use.

### (I) CHEMICAL CHARACTERISTICS

#### (A) Analysis

- (1) Ultimate: C, H, N, S; direct O if possible.
- (2) Proximate: H<sub>2</sub>O, VM, FC, low temperature ash (LTA) and high temperature ash (HTA).
- (3) Maceral analysis: reflectivity.
- (4) Mineral matter and ash: elements as oxides, ash softening and fusion temperatures, mineral analysis, trace element analysis.

*(B) Other chemical properties*

- (1) Caking and agglutinating; coking power.
- (2) Swelling index.
- (3) Plasticity (Gieseler plastometer).
- (4) Thermal mechanical analysis (TMA).

## (II) PHYSICAL CHARACTERISTICS

- (1) Helium density.
- (2) Porosity (Hg intrusion).
- (3) Surface area: N<sub>2</sub>, CO<sub>2</sub> and other fluids.
- (4) Particle size: sieve and sub-sieve.
- (5) Grindability and friability.
- (6) Weathering properties.

## (III) REACTIVITY CHARACTERISTICS

- (1) Thermogravimetric analysis (TGA)/differential scanning calorimetry (DSC).
- (2) Drop tube reactivity.
- (3) Ignition: crossing point; two-headed Fourier transform infrared spectroscopy (FTIR) as well photo acoustic FTIR.
- (4) Pyrolytic behavior: pyrolysis followed by full chromatography analysis.

## FUNDAMENTAL ASPECTS

The reader is directed to five excellent references on the fundamentals of thermal analysis [9–13]. Rajeshwar [8], in his excellent 1983 review, ably discussed the general considerations which control the suitability of TA methods to the study of coal. Some of these considerations are: (1) the heterogeneous nature of the coal; (2) sample geometry; (3) the ambient atmosphere surrounding the sample during TA; (4) the amount and degree of grinding; and (5) the type of sample pretreatment. For example, any non-uniformity in the distribution of the macerals or microlithotypes of a coal will cause variations in enthalpy, weight loss and ultimately the configuration of the thermogram. Sample geometry also affects the result of TA. Particle size, shape and arrangement affect the measured activation energy and kinetics of a coal. These textural parameters physically limit the reaction rate and heat transfer in the sample undergoing TA. Coal possesses a markedly poor heat conductivity; therefore, a thin, uniform layer of a powdered sample should be prepared. If a coherent particle is used, its

dimensions should be small enough to permit uniform heating. In addition, either sample mode should be large enough to be representative of the sample as a whole. This condition is extremely difficult to attain and usually demands many runs of the same sample to characterize a specific coal properly. The amount and degree of grinding must be controlled to prevent selective comminution; for example, vitrinite is brittle and tends to concentrate in the small size fractions, whereas the liptinites (exinites) are more sectile and concentrate in the coarser fractions. Furthermore, coal is susceptible to structural changes which are irreversible when subjected to excessive comminution [8]. Grinding also affects the amount of moisture. It has been observed by Mraw and Silbernagel [14] that the amount of water that can be replaced after heating (110°C) and drying coal varies according to rank (i.e.,  $\approx 100\%$  in the high-volatile bituminous Herrin No. 6 coal,  $\approx 60\%$  in the sub-bituminous Rawhide coal and  $\approx 35\%$  in an Arkansas lignite). These authors suggest that this loss of water reflects a change in pore structure in these coals on preheating. It becomes apparent, therefore, that any pre-treatment of coal is undesirable because it might alter the original characteristics of the coals under investigation. Sample storage prior to testing is also a critical factor because coals can readily auto-oxidize; therefore, it is most desirable to store the samples in an inert gas, preferably argon and not nitrogen, because nitrogen affects the agglomerating properties of the coal. A coal sample exposed to thermal analysis should have controlled surroundings; for example, if the sample is encapsulated by a deep cup-shaped holder, it might be exposed to a self-generated atmosphere which will alter the trace of the thermogram because it is not in contact with the ambient atmosphere [15]. If the intended atmosphere is to be strongly oxidative, any limitation in the rate of oxygen supply to the reactant will change the behavior of the reaction from exothermic to endothermic. Some of the controversy about the early DTA data on coal might be related to such an aberrant behavior [16]. From the above discourse it becomes apparent that one of the most important factors in TA is the ease with which effluent gases can escape from the reaction zone. The time taken for the effluent gases to escape is governed by sample geometry, particle size, sweep gas flow rate and the heating rate selected for thermal analysis. The longer the residence time, the more complex will be the effects of the recondensation and secondary reactions. A high sweep-gas flow rate and a moderate heating rate ( $\approx 10^\circ\text{C min}^{-1}$ ) will tend to decrease the spurious effects just discussed.

## CHEMICAL ANALYSIS

### *Proximate analysis*

Proximate analysis of coal includes the determination of its moisture, volatile matter, fixed carbon and ash contents. These coal parameters have

long been determined by ASTM methods (D-3172) which are tedious and time-consuming. During the past eight years, TG techniques have provided a rapid and convenient method to replace the classical ASTM procedures [17–22]. Fyans [17] originally used a combination of non-isothermal and isothermal techniques for proximate analysis. In this method oxygen was swept into the system after the sample was heated programmably in an inert atmosphere. This technique permitted the evolved water and volatile matter to be measured. The devolatilized coal then was heated isothermally to 950°C for 7 min allowing the fixed carbon and ash contents to be determined. Fyans, however, noted that this method was not without controversy. Thermogravimetry experiments use small samples, usually less than 1 g, and with some TG systems even less than 10 mg of sample. Because ASTM methods specify a much larger sample (> 1 g), skeptics question the capabil-

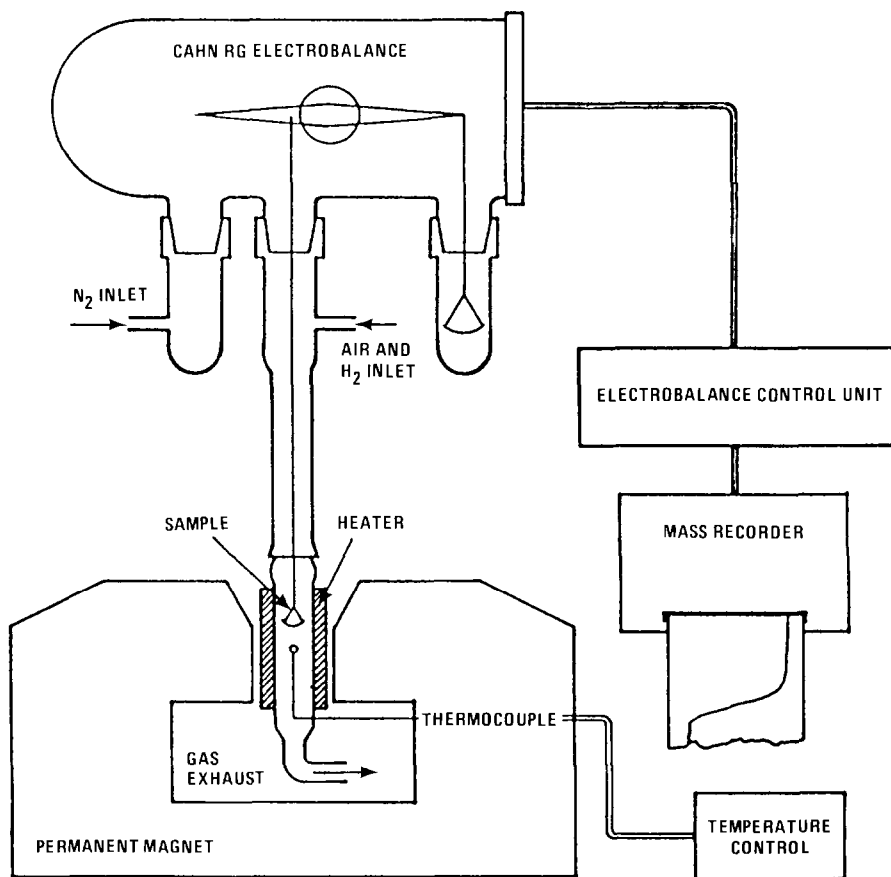


Fig. 1. Diagram of a TMG balance for continuous measurement of the weight change of a coal as it is heated. (From Rowe and Human [24], p. 57).

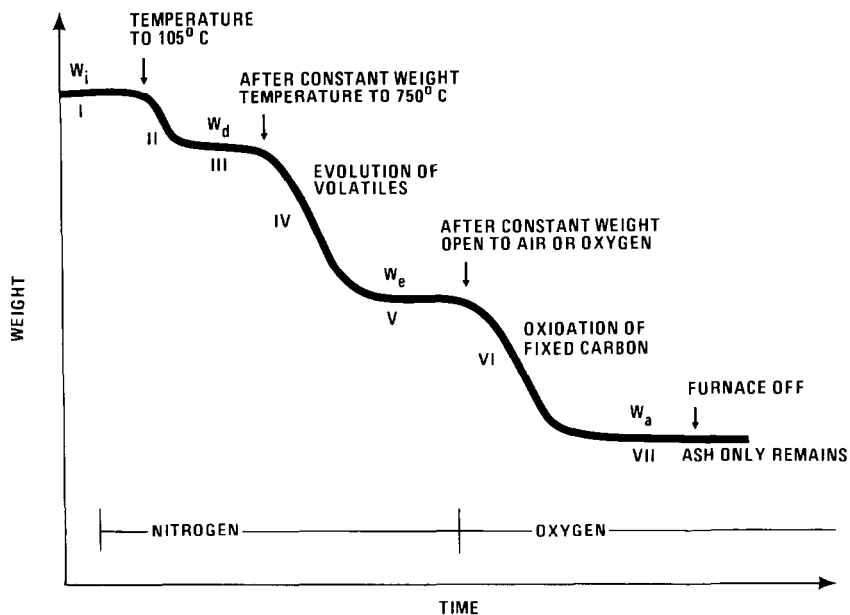


Fig. 2. Diagram illustrating the change in weight of a sample as the temperature and atmosphere is altered. (From Rowe and Hyman [24], p. 58).

ity of TG systems to conform to the requirements of D-3172 for repeatability and reproducibility.

Rosenvold et al. [18] used two consecutive non-isothermal techniques to determine the proximate analyses of bituminous coals from Ohio. More recently, several investigators [23,24] proposed a combined thermogravimetry-thermomagnetometry (TMG) method as an alternative for measuring the pyrite content of coal in addition to proximate analysis. TMG equates the pyrite content of the coal to the amount of easily oxidizable and reducible iron compounds which occur in the coal. In this method a thermomagnetic balance is employed (see Fig. 1). The pyritic sulfur is determined by using a magnet with pole faces shaped for Faraday analysis. A sample is placed in a quartz or platinum holder suspended from the balance into a furnace. This system can also control the flow of pure  $N_2$ ,  $H_2$  and air or  $O_2$ . Initially, the system is flushed with dry nitrogen for at least 10 min at a flow rate of  $50 \text{ cm}^3 \text{ min}^{-1}$  to purge the unit of oxygen. The unit is then ready to begin the proximate analysis.

Figure 2 shows schematically the operations necessary to obtain the proximate analysis from TG with continuous  $N_2$  flow. The initial weight is recorded in region I, after which the furnace temperature is increased to  $105^\circ\text{C} \pm 5^\circ\text{C}$  to evolve the moisture, seen as the weight loss in region II. After 5–10 min the weight becomes constant yielding a dry weight,  $W_d$ , in region III. The temperature is held for 7 min at the elevated temperature

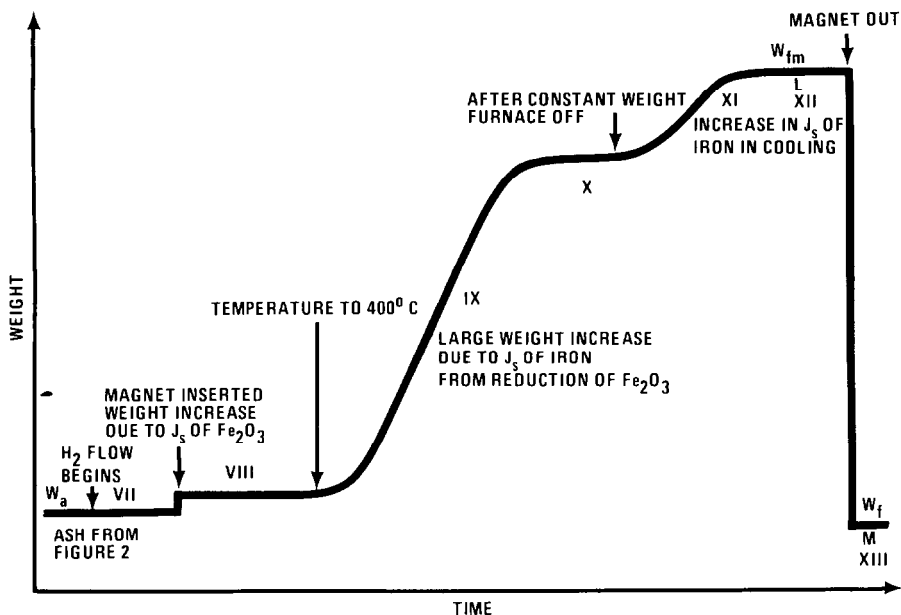


Fig. 3. Diagram illustrating the change in apparent weight (magnetic attraction) of a sample as iron oxide in the ash is reduced by  $H_2$  at elevated temperatures. (From Rowe and Hyman [24], p. 58).

(750–950°C), again with a constant weight being attained in region V ( $W_c$ ). This weight loss (IV) permits the direct calculation of volatile matter. At V, air or oxygen is permitted to flow through the system at a rate of  $50 \text{ cm}^3 \text{ min}^{-1}$ , which oxidizes the remaining organic matter yielding the weight loss seen in region VI. This weight loss (VI) represents the direct measurement of fixed carbon, whereas in the ASTM method fixed carbon is determined indirectly by difference. When ash alone is left, the weight again becomes constant,  $W_2$  (VII), and the heat is shut off. After cooling to  $\sim 150^\circ\text{C}$ ,  $H_2$  is passed through the system at  $50 \text{ cm}^3 \text{ min}^{-1}$  at the beginning of the analysis for pyrite content. As with the elevated temperatures (750–950°C) in region III, the temperature is not critical. Furthermore, neither is the exact rate of gas flow important.

After at least 10 min of  $H_2$  flow, a magnet is placed in the system so that it acts on the sample; this results in an apparent weight increase as shown in Fig. 3 in region VIII. This increased weight is due to the attractive force of  $\gamma\text{-Fe}_2\text{O}_3$ —the oxidation product of pyrite. The temperature of the system is then raised to  $400^\circ\text{C}$  (again the exact temperature is not critical) with  $H_2$  flowing, thus causing the  $\gamma\text{-Fe}_2\text{O}_3$  to be reduced to metallic iron. This yields a large apparent weight increase (see region IX) because the magnet attracts iron more strongly than it does  $\gamma\text{-Fe}_2\text{O}_3$ . When the reduction is complete, the apparent weight once again becomes constant (see region X) and the



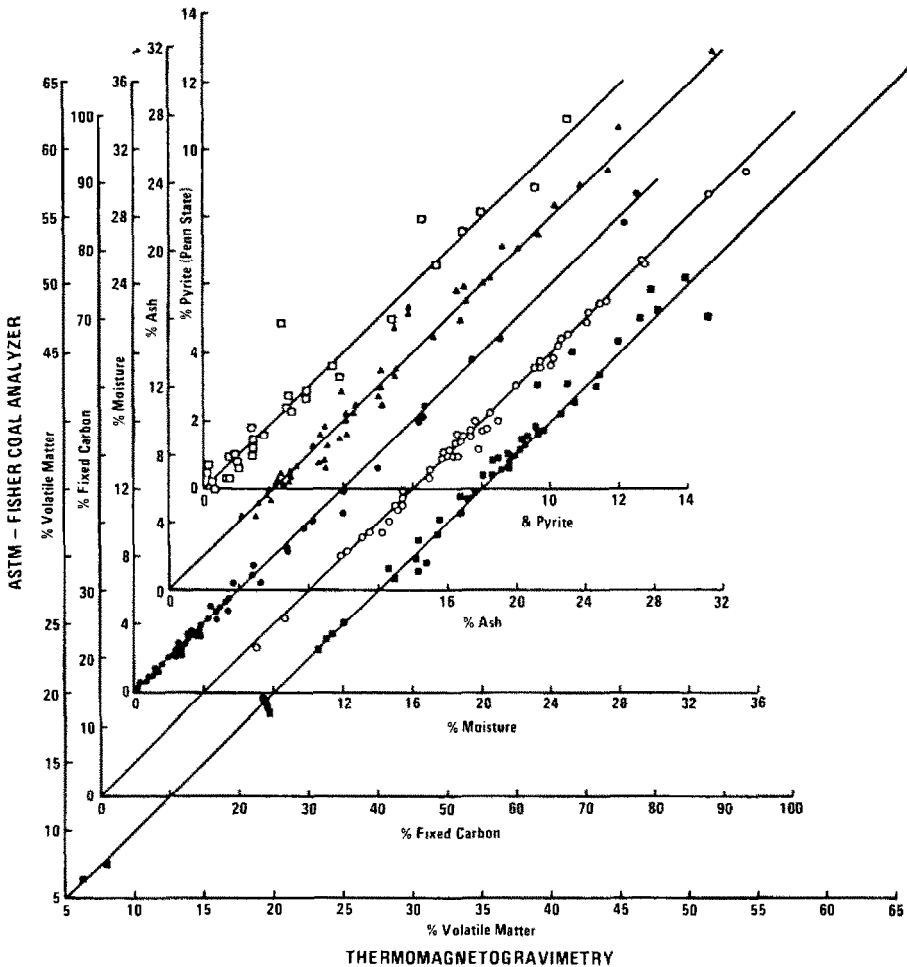


Fig. 4. Graphic results from the TMG technique for the measurement of proximate analysis and pyrite content as compared to ASTM values measured on the same samples. (From Rowe and Hyman [24], p. 58).

heat is turned off. On cooling, the weight increases (region XI) until the sample reaches room temperature (XII), when the magnet is removed and the weight of the residue is recorded as  $W_f$  (region XIII). The pyritic sulfur content is then calculated as percentage of  $\text{FeS}_2$  from the apparent weights on the thermogram by the formula:

$$\% \text{ Pyritic sulfur} = \frac{W_{fm} - W_f}{218} \times \frac{119.85}{55.85} \times \frac{100}{W_d}$$

Figure 4 illustrates the reproducibility of this TMG method for the proximate analysis and pyrite content determination of coals by comparing the results of this technique with those derived from ASTM methods on the

same coals. The agreement appears to be good in each analysis because the four components define a 45° line with relatively small scatter. The use of TMG has several advantages over current ASTM methods. They are: (1) simplicity and speed of analysis; (2) low cost; (3) potential for automation and computer control; and (4) widespread availability of the apparatus.

### *Rank and maceral analyses*

Glass [25] observed, in DTA traces (see Fig. 5) of bituminous coals, three major endotherms: the first peak at 150°C, the second at 350–550°C and the third at 600–700°C. According to Van Krevelen [26], the first peak is related to the removal of water, the second refers to primary devolatilization and the third reflects secondary degasification.

Study of these DTA traces illustrates that details of the curve disappear with increased rank; for example, the semi-anthracites and anthracites do not exhibit primary devolatilization, whereas bituminous coals exhibit a doublet which represents primary and secondary endothermic devolatilization. These two degasification peaks are separated by an exothermic peak which probably represents an intermediate resolidification which reflects condensation of the aromatic components of the coal.

Kroger and Pohl [32] studied the thermal behavior of various pure macerals (see Fig. 6). They concluded that the reactions are endothermic except between 440 and 550°C, the range representing the occurrence of increased aromaticity and chemical condensation.

When the results of vacuum DTA (Fig. 7) and normal DTA are compared, a marked dichotomy occurs which is not easily explained and possibly refutes DTA as a method for characterizing coal. Two authors, Boyer and Dayen [33], hypothesized that the exothermic reaction between 400 and 500°C reflects the rapid increase in thermal conductivity at the time when agglutination of the grains of coal occurs. In contrast, Gaines and Partington [34] suggested that the endotherms obtained by normal DTA are partly due to the coal possessing a lower thermal diffusivity than the inert materials and to the absorption of latent heat by the volatile products. In contrast, the pyrolytic reactions were found to be predominantly exothermic up to 500°C.

Vacuum DTA was utilized by Whitehead and his co-researchers [27–31]. They recognized that coals of different rank (lignite through semi-anthracite) exhibit exotherms that move towards higher temperatures as the rank increases. The exothermic peaks represent pyridine-extractable material. These researchers also made DTA runs on the different microlithotypes; they found that vitrain and clarain showed no marked difference, whereas durain showed a diminished exotherm and fusain showed no marked peaks and appeared to be essentially inert. Spores yield sharp peaks, and resin gives broad peaks. Whitehead et al. [27–31] also observed that TA helped to

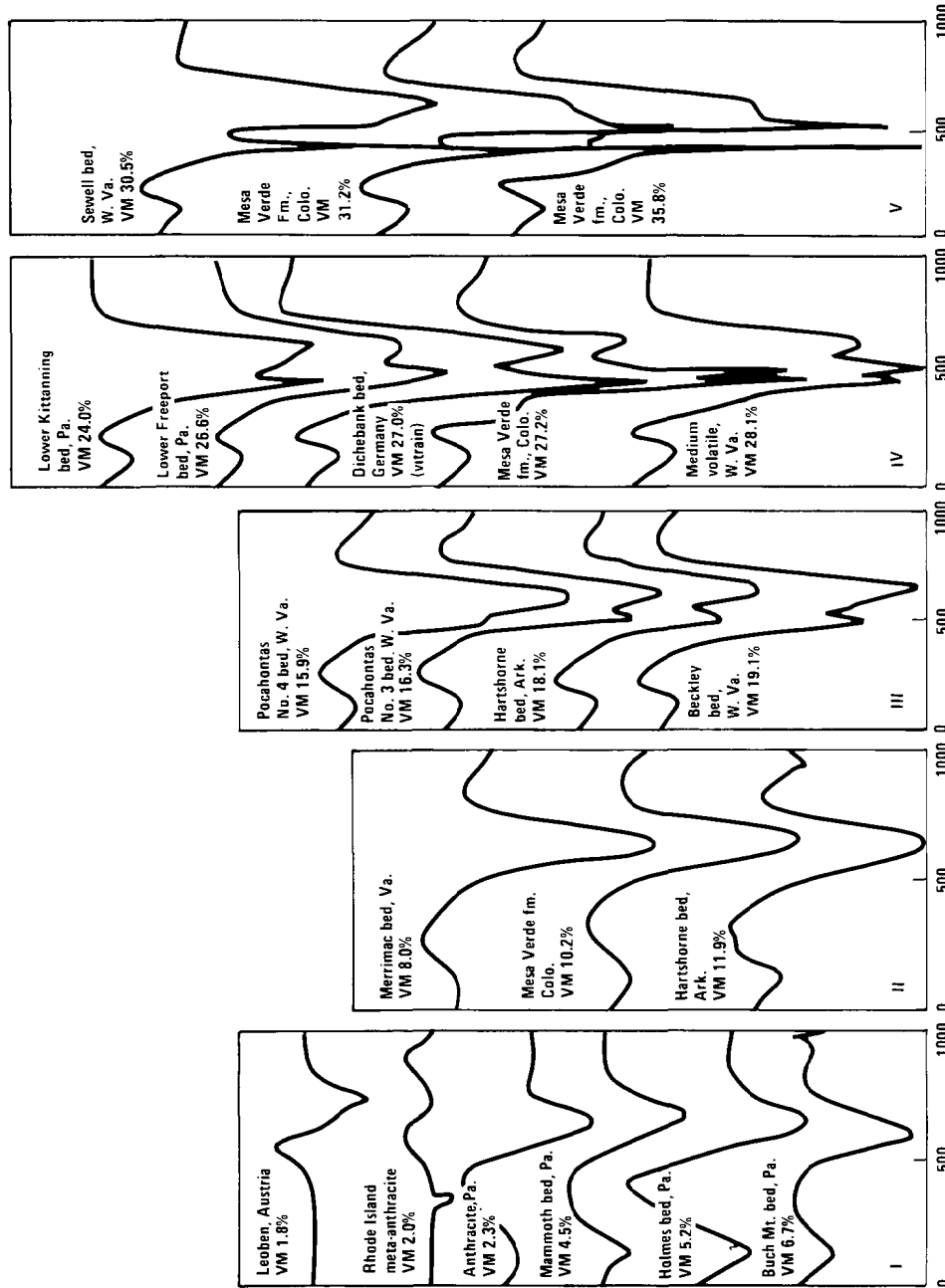


Fig. 5. Differential thermal analysis traces of coal. (I) Meta-anthracites and anthracites; (II) semi-anthracites; (III) low volatile bituminous coals; (IV) medium volatile bituminous coals; and (V) high volatile A bituminous coals. VM = percentage volatile matter content. (From Glass [25], p. 294).

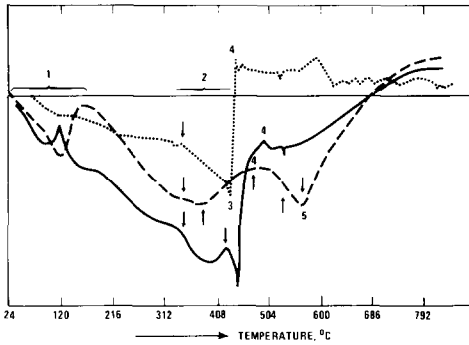


Fig. 6. DTA traces of macerals from seam "Zollverein". Vitrinite (—); exinite (·····); micrinite (- - - - -). (Modified from Kroger and Pohl [32]).

detect cellulose, if present, in lignites resulting in a doublet exotherm with cellulose decomposition occurring at about 400°C preceding lignite carbonization at about 425°C.

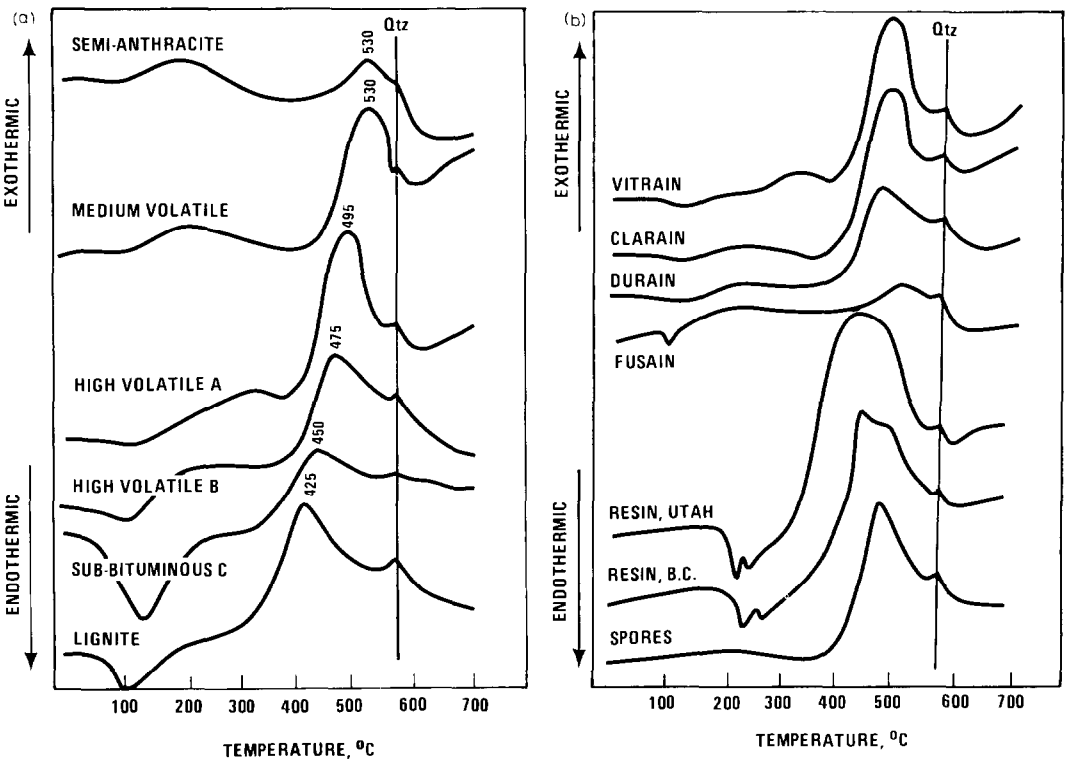


Fig. 7. (a) Vacuum DTA trace of vitrains of various ranks of coal. (From Whitehead et al. [27-30]). (b) Comparison of DTA traces of vitrain, clarain, durain, fusain, resin and spores. (From Whitehead et al. [27-31].)

More recently, Mahajan et al. [35] and Rosenvold et al. [18], using DSC in  $N_2$  inert atmosphere, concluded that the thermal behavior of bituminous coals is completely endothermic! However, Mahajan et al. [35] noted that exotherms occur in lower rank sub-bituminous and lignitic coals. Rosenvold et al. [18] suggest that DSC methods may be a more effective indicator of coal rank in contrast to earlier DTA studies which yielded conflicting results [25,27–33]. A profound paper by Elder and Harris [36] reports on their observations of a combined TG/DSC study of the six most abundant bituminous coals from Kentucky. They summarized that the higher ranked East Kentucky coals show less thermal behavior, or nearly featureless, normalized heat-flow curves compared to those from West Kentucky. They interpret the DSC scans and their normalized heat-flow curves as follows. After the endothermic loss of residual moisture on the normalized heat-flow curves, there is a small endotherm at about 200–350°C where all the coals start to lose small amounts of pyrolytic water from the decomposition of phenolic structures, and oxides of carbon from carboxyl and carbonyl groups. These broad, shallow endotherms are not easy to quantify. At about 350°C primary carbonization starts with the release of  $CO_2$  and  $H_2$ . On increased temperature,  $CH_4$  and other lower aliphatics are evolved along with  $H_2$ , CO and alkyl aromatics. The rupture and breaking of the aliphatic and hydroaromatic bonds provide sufficient energy for the competing endothermic devolatilization of condensable oils and tars. The overall effect is exothermic with a maximum heat flow in the region 425–450°C depending on the heating rate.

#### *Mineral matter and ash*

Warne [37] and Earnest [38] authored excellent references on the thermal analysis of minerals in coal. In addition, two very recent DTA articles discuss, respectively, the decomposition at 400 and 575°C of anhydrous carbonate minerals in coal and in related fuels [39], and oxidative profiles for pyrite in low temperature ash (LTA) components of coal [40]. The first article studied the DTA/TG of siderite ( $FeCO_3$ ), rhodochrosite ( $MnCO_3$ ) and magnesite ( $MgCO_3$ ) as they decompose during heating. The temperatures of the decomposition peaks were recorded in inert gases such as  $N_2$  or  $CO_2$ . The second article defined the oxidative thermal curves for pyrite, marcasite and several low temperature ashes (LTA). In addition synthetic mixtures of pyrite, ferrous sulfate monohydrate and alumina were tested to study the effect of ferrous iron sulfates on the DTA oxidative profiles. It was learned that the presence of iron sulfate lowers the peak temperatures and forms a doublet in the oxidative profiles. Furthermore, thermograms of pyrite, as well as of the LTA that contained significant concentrations of iron sulfates, exhibited endothermicity between 630 and 670°C. This event is characteristic of the sulfate component. In contrast, this event was absent

in pyrite which contained no sulfate. It is important to note that the presence of iron sulfates in the LTA at about 660°C masks the less intense dehydroxylation endotherm of the mixed-layered clays which contained smectite clay minerals.

#### OTHER CHEMICAL/PHYSICAL PROPERTIES

Plasticity and dilatation in Gieseler plastometry are strongly dependent upon the rank and petrographic composition of a coal. An increase in rank will shift all the diagnostic peaks to higher temperatures, whereby the maceral composition will change the thermal response of the coal. For example, inertinites exhibit no plasticity on heating, whereas liptinites/exinites become extremely fluid and vitrinites exhibit an intermediate position. Krevelen et al. [41] stated that in mixtures of vitrinites and liptinites of the same rank, the logarithm of the fluidity behaves as an additive quantity, whereas a non-softening constituent, such as mineral matter or an inertinite, exhibits strong depressing effects on fluidity.

#### *Dilatometric-TMA measurements*

The results of dilatometric and/or TMA measurements are similar to those of plasticity studies. If coal is heated to a constant temperature the

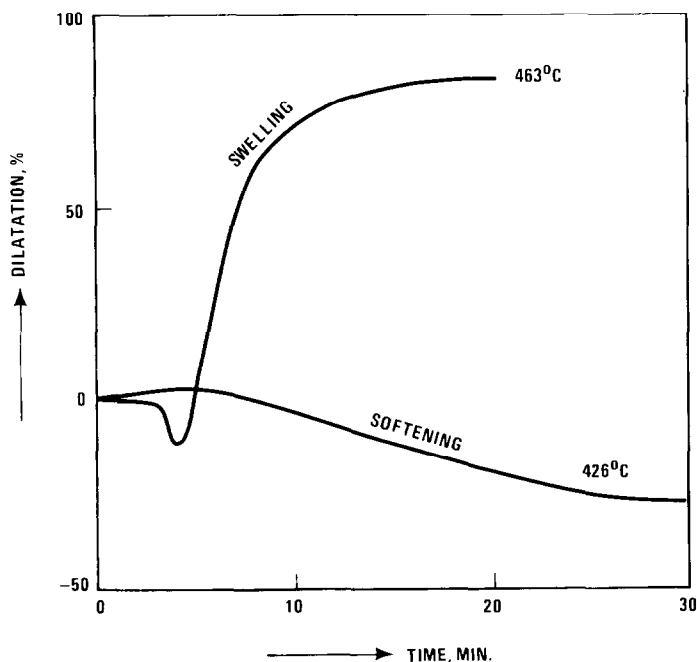


Fig. 8. Dilatation of a semi-bituminous coal at constant temperature. (From Van Krevelen [26], p. 276).

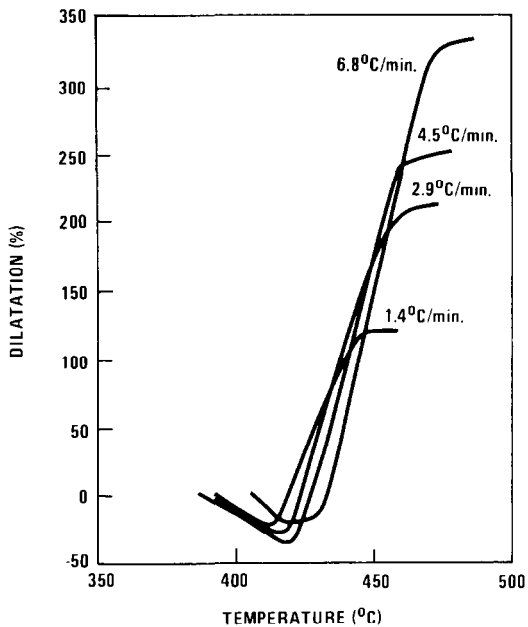


Fig. 9. Effect of heating rate on the dilatation of a bituminous coal. (From Van Krevelen [26], p. 276).

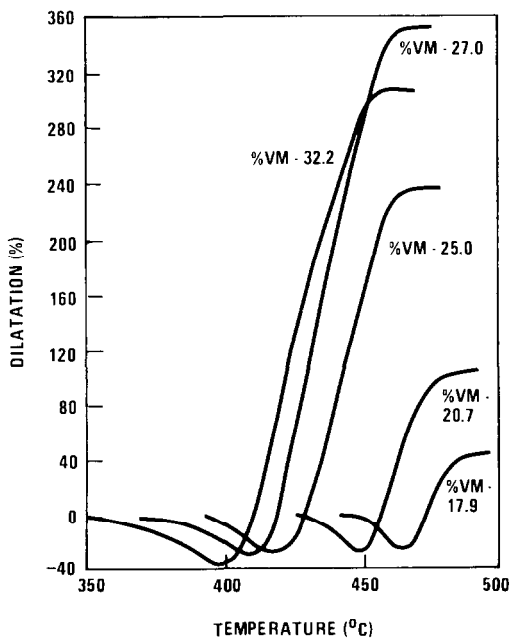


Fig. 10. Dilatometer curves of coal of different rank. % VM = percentage volatile matter. (From Van Krevelen [26], p. 276).

## EXPERIMENTAL TECHNIQUES

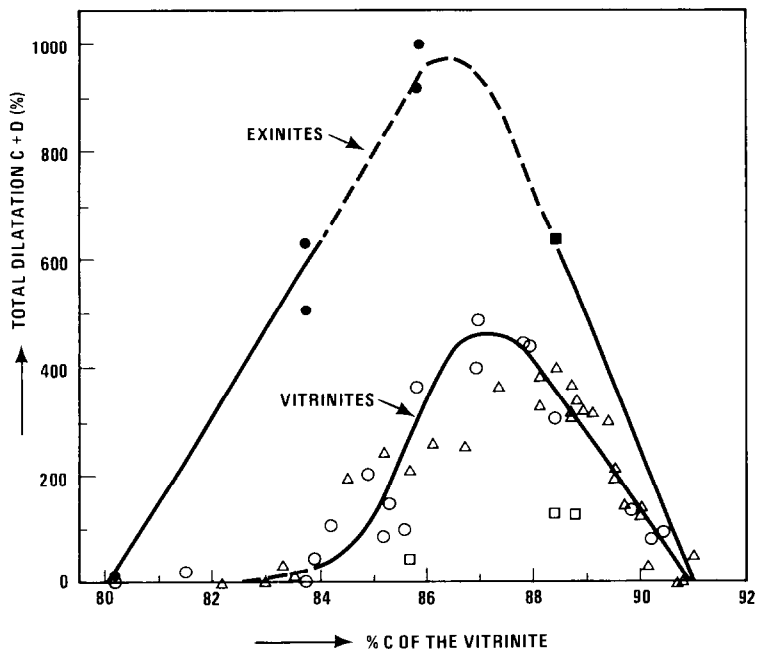


Fig. 11. Dilatation of vitrinite and exinites. (From Van Krevelen [26], p. 277).

shape of the dilatometric curves depends on the temperature level: if the temperature is relatively low, only softening occurs; if the temperature is relatively high, it is followed by swelling (see Fig. 8). If the coal is heated at a constant rate during dilatation, a typical curve is constructed. If the rate of heating is increased, the points along the curve are shifted towards a higher temperature and the percentage of dilatation increases. As the rank increases, the dilatation reaches its maximum at above 87% carbon and 30% volatile matter (see Figs. 9 and 10).

As stated earlier, the dilatometric curve is very sensitive to the type of maceral; for example, inertinites do not soften and, therefore, do not exhibit dilatation. Liptinites/exinites possess a very strong dilatation with vitrinites occupying an intermediate position [42] (see Fig. 11). The total dilatation of the softening components is an additive phenomenon within the range of simultaneous softening [43]. Non-softened constituents (inerts) exert a depressing effect which is, in part, controlled by the particle size of these components (i.e., the smaller the size the greater the effect).

Characteristic plastometric temperatures during carbonization of coals of different rank are shown in Fig. 12. These data were accrued with a constant heating rate of  $3^{\circ}\text{C min}^{-1}$ . This figure illustrates that the residence time of the plastic phase is longest for the vitrinites at a carbon content of 87.5%



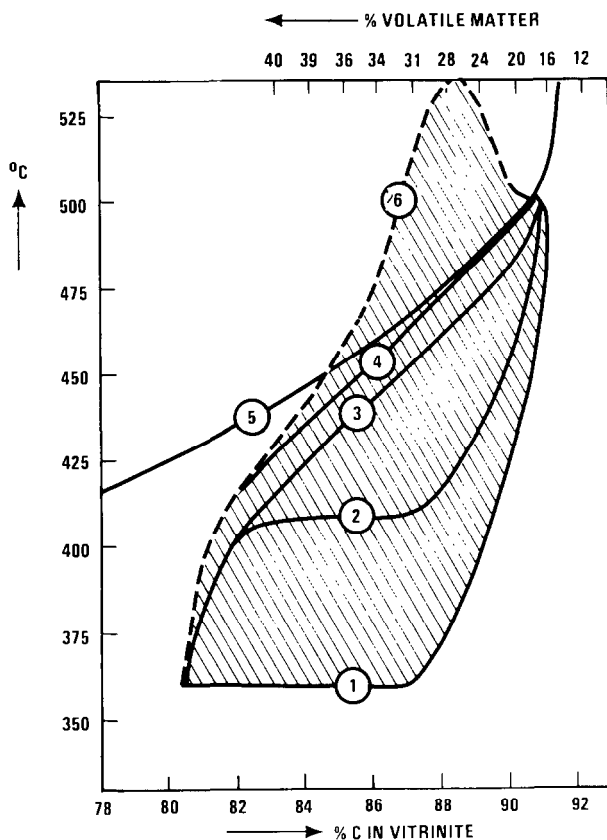


Fig. 12. Characteristic temperatures in carbonization. (1) Softening; (2) beginning of swelling; (3) maximum fluidity; (4) end of swelling; (5) maximum rate of devolatilization; (6) resolidification. (From Van Krevelen [26], p. 278).

(VM about 29%). The line of maximum plasticity (fluidity) runs almost parallel with maximum swelling, whereas the latter nearly coincides with that of the maximum devolatilization rate.

Vitrinites exhibit no plastic behavior if their carbon content is lower than 80.5% or more than 91%. For liptinites/exinites of equal rank the same is true; however, the degree of fluidity in the plastic zone is much higher than that in the corresponding vitrinites.

#### *DSC/TG*

The specific heats ( $C_p$ ) of bituminous and sub-bituminous coals were measured over a temperature range 300–360 K [44]. It was observed that  $C_p$  of the coals were dependent on particle size, temperature, rank, moisture content and the type of pre-treatment applied to the coal. For example, it is important to know if the coal was wet or dry sieved. The results of this work

only showed a minor difference in the specific heat between the sub-bituminous and the bituminous coals.

### *Kinetics / reactivity*

Thermogravimetry is widely applied to determine rate processes in coals [45]. This method involves a continuous measurement of the change in mass or rate of mass loss (DTG) of a sample with temperature (or time). Kinetic parameters, such as activation energy and order of reaction, can be gleaned from these types of data. Several methods have been developed to permit the kinetic analysis of TG data. Kinetic parameters by this method were calculated from one TG curve obtained at a constant heating rate. These types of calculations are frequently challenged because the kinetic properties are influenced by heating rate and are thought to yield incorrect values for activation energy and reaction order. It is also believed by the skeptics that it is necessary to calculate these parameters using data derived from multiple heating rates if reliable results are to be obtained. In this work the author compared four methods for analyzing TC data of a sub-bituminous coal. It was concluded that the methods using only one heating rate were superior because they do not require any temperature correction and are linearly related to the shape factor,  $S$ , which is a measure of the asymmetry of a zone or reaction. If these plots are constructed for a range of experimental conditions, they may be used to calculate an activation energy from the shape factor measured from the thermogram under these conditions. This is an additional attractive feature of methods requiring one heating rate.

Cummings [46] employed a burning profile test to assess coal reactivity where the derivative thermogravimetric (DTG) output from a thermobalance system is plotted versus temperature as the coal is heated at a constant rate in a flowing air stream. A profile is produced, characterized by several features, the importance of which is the peak temperature, or temperature at which the sample loses weight at the maximum rate. A high peak temperature is indicative of a less reactive fuel. During the test, 4 datum temperatures (see Fig. 13) are measured on the burning profile curve: (a) the first initiation temperature where the weight begins to fall (ITVM); (b) the second initiation temperature where the rate of weight loss accelerates due to the onset of combustion (ITFC); (c) the peak temperature as described (PT); and (d) the burnout temperature, where the weight becomes constant at completion of burning (BT).

Before beginning this study of coals, Cummings considered it necessary to assume that the combustion process in the burning profile test approximates first-order kinetics. To avoid complications due to weight losses by devolatilization during the early stages, isothermal thermogravimetric runs were carried out on samples of coke prepared by the separate devolatilization of 1-g aliquots of bituminous coals in an inert atmosphere at 900°C (coke

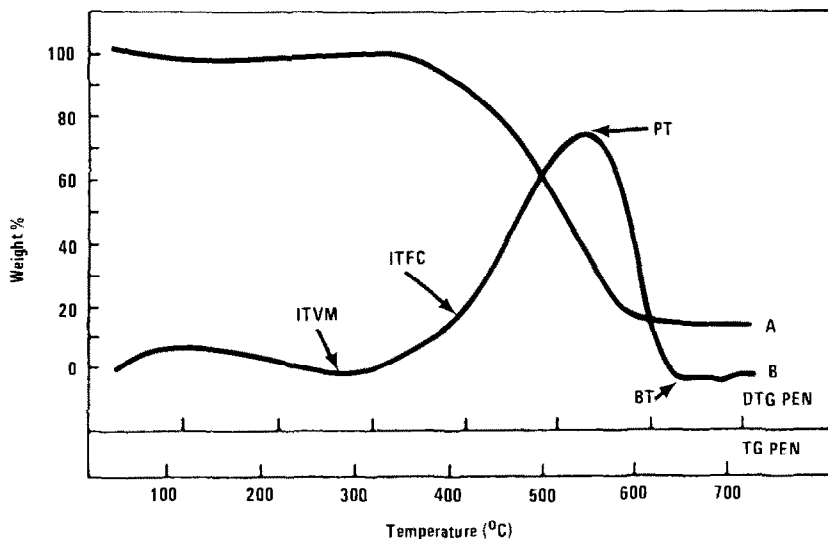


Fig. 13. Typical burning profile/TG curves for bituminous coal: (A) TG trace, (B) DTG. (From Cummings [46], p. 1436).

“A”). If the reaction is of first order, plots of  $dW/dt$  versus  $W$  (the weight unburned) should be linear, and this is shown to be approximately true by the results presented in Fig. 14. Having established this fact for the coke

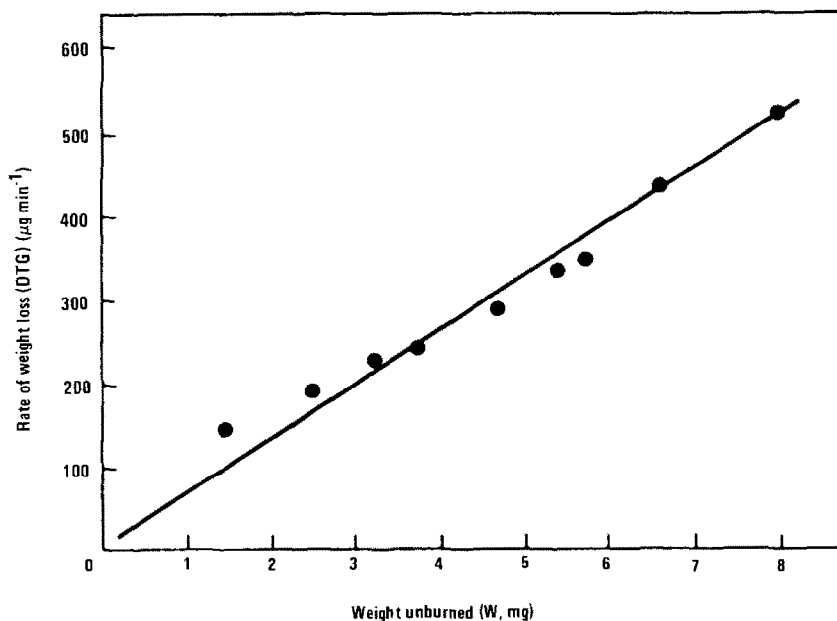


Fig. 14. Isothermal burning plot for a coke at 505°C. (From Cummings [46], p. 1437).

samples, Cumming felt it justifiable to continue to assume first-order kinetics for the burning of coals, and to employ the following equations in calculating values of the specific reaction rate:

$$K = (dW/dt)W^{-1}$$

where  $dW/dt$  is the instantaneous rate of weight loss;  $W$  the weight of unburned combustible; and  $K$  the specific reaction rate.

The specific reaction rate is related to temperature by the Arrhenius equation:

$$K = A \exp(-E/RT)$$

or

$$\log K = \log A - E/2.303RT$$

where  $A$  is the frequency factor;  $E$  the activation energy;  $R$  the universal gas constant; and  $T$  the absolute temperature.

Figure 15 shows a combined TG/DTG plot for an anthracite. The burning profile of the DTG curve exhibits a typical peak temperature at 650°C. From the TG/DTG curves a series of  $K$  values were calculated at 25°C intervals. These values were used along with the corresponding absolute temperature to calculate the  $X$  (temperature) and  $Y$  ( $\log K$ ) coordinates of the Arrhenius plot as listed in Table 1.

The Arrhenius plot shown in Fig. 16 for the anthracite displays two regions of linearity: 350–500°C and 500–725°C. From the gradients of

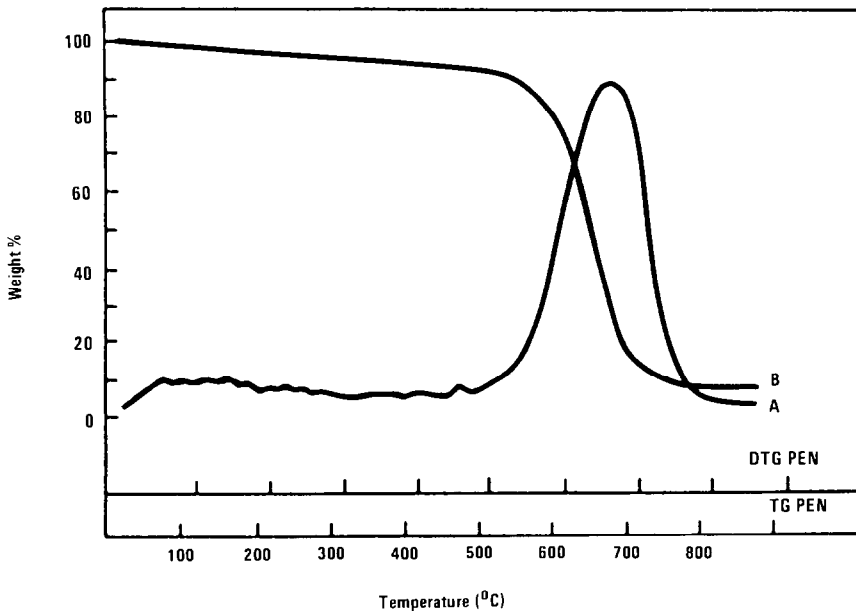


Fig. 15. TG/DTG traces for anthracite: (A) DTG; (B) TG. (From Cummings [46], p. 1438).

TABLE 1  
Calculation of Arrhenius coordinates for anthracite <sup>a</sup>

Temp., $T$ ( $^{\circ}\text{C}$ )	$1/T_{\text{abs}}$ $\times 10^{-3}$	Weight unburned (mg)	$dW/dt$ ( $\mu\text{g min}^{-1}$ )	$K$ ( $\text{s}^{-1}$ )	$\log K$
$X$					$(Y)$
350	1.61	17.50	12	$6.92 \times 10^{-4}$	-3.16
400	1.49	17.45	24	$1.38 \times 10^{-3}$	-2.86
425	1.43	17.35	30	$1.73 \times 10^{-3}$	-2.76
450	1.38	17.30	42	$2.43 \times 10^{-3}$	-2.61
475	1.33	17.20	60	$3.49 \times 10^{-3}$	-2.46
500	1.29	17.10	90	$5.26 \times 10^{-3}$	-2.28
525	1.25	16.90	160	$9.47 \times 10^{-3}$	-2.02
550	1.22	16.55	318	$1.92 \times 10^{-2}$	-1.72
575	1.18	16.00	660	$4.13 \times 10^{-2}$	-1.38
600	1.15	14.60	1320	$9.04 \times 10^{-2}$	-1.04
625	1.11	12.40	1896	$1.53 \times 10^{-1}$	-0.82
650	1.08	9.10	2076	$2.28 \times 10^{-1}$	-0.64
675	1.05	5.90	1932	$3.27 \times 10^{-1}$	-0.48
700	1.03	2.80	1416	$5.06 \times 10^{-1}$	-0.29
725	1.00	1.10	756	$6.97 \times 10^{-1}$	-0.16

<sup>a</sup> Sample weight, 20.0 mg; moisture content, 2.5 wt%; ash content, 8.5 wt%; weight of combustible, 17.8 mg.

these lines the apparent activation energies associated with the two regions are calculated as 52.8 and 149.3  $\text{kJ mol}^{-1}$ , respectively. Although these values define the apparent activation energies associated with the various stages of combustion, they say nothing about the overall reactivity of the fuel, because they do not incorporate any term relating to the amount of sample reacted during each stage. Cummings [46] met this requirement by utilizing the concept of a weighted-mean apparent activation energy ( $E_m$ ) as defined in the equation:

$$E_m = F_1 E_1 + F_2 E_2 + \dots F_n E_n$$

and calculated as follows:

Weight loss over the first region of Arrhenius linearity (i.e., 350–500 $^{\circ}\text{C}$ ) = 0.4 mg or 2.2%, i.e.,  $F_1 = 0.022$ , hence  $E_1 F_1 = 1.2 \text{ kJ mol}^{-1}$

Weight loss of second region (500–725 $^{\circ}\text{C}$ ) = 16 mg or 89.9%, i.e.,  $F_2 = 0.899$ , hence  $E_2 F_2 = 134.2 \text{ kJ mol}^{-1}$  and  $E_m = 1.2 + 134.2 = 135.4 \text{ kJ mol}^{-1}$

TG/DTC curves and the Arrhenius plot for a typical bituminous coal are shown in Figs. 17 and 18.

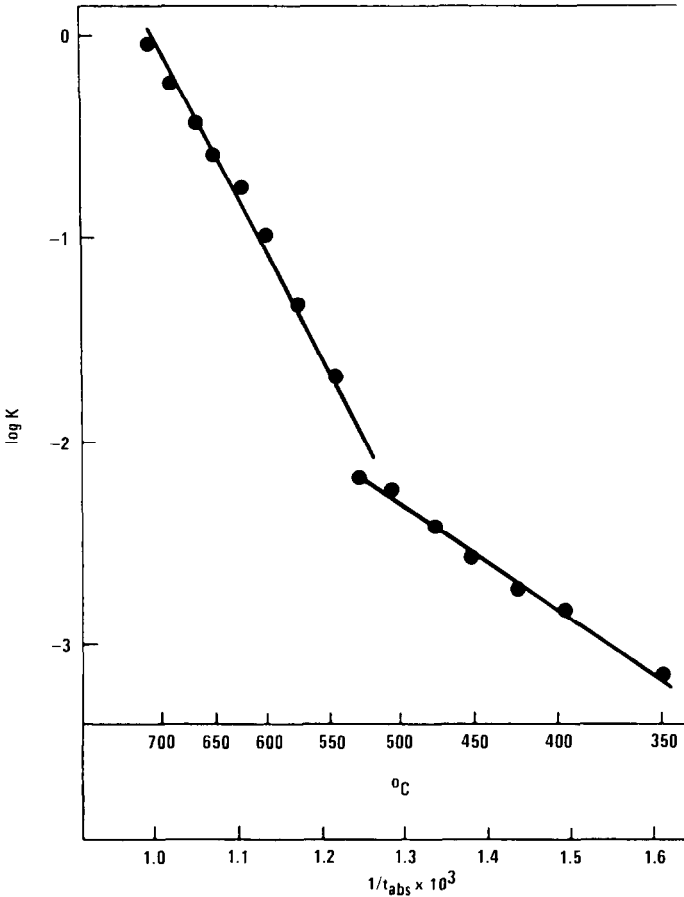


Fig. 16. Arrhenius plot for anthracite. (From Cummings [46], p. 1438).

Cummings [46] applied the same treatment as for the anthracite to bituminous coal. He obtained the following values ( $\text{kJ mol}^{-1}$ ):

$$E_1 = 96.9 \quad F_1 = 0.029$$

$$E_2 = 41.8 \quad F_2 = 0.180$$

$$E_3 = 96.1 \quad F_3 = 0.763$$

hence  $E_m = 83.6$

This treatment was then repeated for 22 samples of coal of various rank, petroleum coke and wood charcoal. The resulting values for  $E_m$  are given in Table 2.

Cummings [46] concluded that for the 22 coals and other solid fuels studied, there is a definite correlation between reactivities as assessed by the burning-profile peak temperature and by the weighted-mean apparent

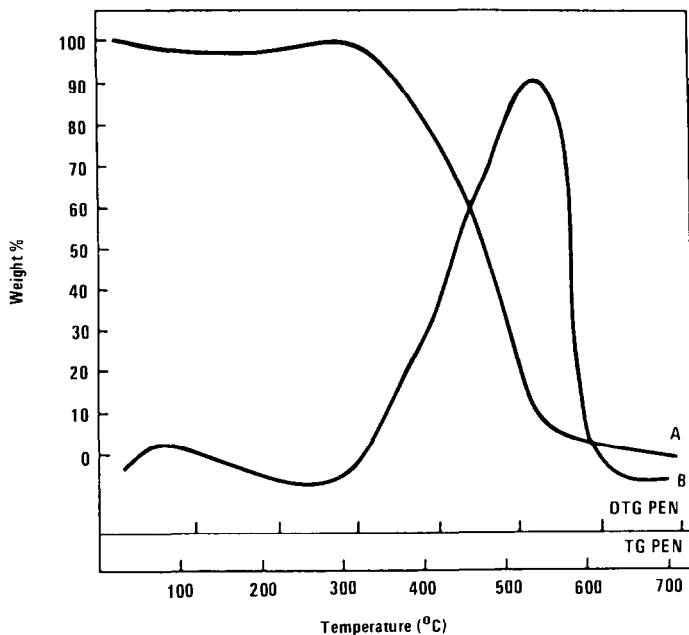


Fig. 17. TG/DTG plot for bituminous coal: (A) TG; (B) DTG. (From Cummings [46], p. 1439).

activation energy ( $E_m$ ) (see Fig. 19). In several instances this method gives results at variance with the previously accepted datum temperature method, but he suggests that  $E_m$  is a more reliable and scientifically based means of assessment.

Serageldin and Pan [47] developed a linear relationship between procedural activation energy and heat of reaction when used as catalysts in the presence of alkali metal salts. They concluded that: (1) alkali metals increased, (a) overall coal decomposition and (b) CO emission; (2)  $\text{Li}_2\text{CO}_3$  was the most effective catalyst in all atmospheres; (3) mixed catalysts are more effective than single catalysts; (4) a relationship between heat of reaction and activation energy exists; and (5) the decrease in activation energy did not always reflect an increase in coal reactivity.

Structural changes in coal chars during gasification were studied in bituminous coal chars of the same rank [48]. These chars were gasified at atmospheric pressure with  $\text{CO}_2$  at  $980^\circ\text{C}$ . Porosities and reaction rates were measured at different degrees of carbon burn-off. A comparison of changes in porosity and reactivity with percentage burn-off indicates that the total surface area is a significant parameter for reactivity but cannot be regarded as the major controlling factor. It was observed by De Koranyi and Williams [48] that two chars of the same rank exhibited remarkably different reactivities. The different shapes of the reactivity plots indicate differences in

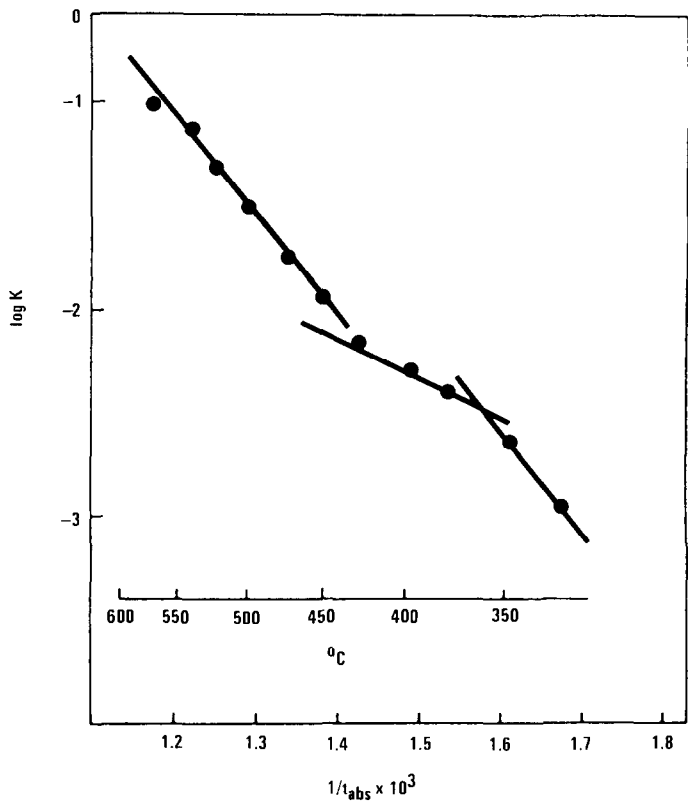


Fig. 18. Arrhenius plot for bituminous coal. (From Cummings [46], p. 1439).

structure and changes in reactivity. They further observed that changes in reactivity plots are only partially paralleled by surface area changes in the char. It appeared that an active surface area may be important in controlling reactivity. A constant flat area after the maximum is reached in the reactivity curve indicated a constant dispersion of active sites. A decrease in reactivity after the maximum is reached indicated either: (1) a decrease in active site dispersion; or (2) a decline in activity of active sites with burn-off. De Koranyi and Williams observed ambiguity in the porosity results, especially toward the end of gasification which they related to a complex reaction between structure, reactivity and other effects, such as the catalytic effect of inherent mineral matter. They also observed that there appears to be a continuum of all types of pores throughout the chars up to nearly full conversion.

*Multiple systems: TG/MS, TG/GCS/MS, etc.*

Thermogravimetry (TG) and mass spectroscopy (MS), using a vacuum microbalance coupled with infrared spectroscopy, were employed to study



TABLE 2

 $E_m$  values and burning profile peak temperatures for 22 solid fuels

Sample No.	Volatile matter (wt%, daf <sup>a</sup> )	Type	Peak temp. (°C)	$E_m$ (kJ mol <sup>-1</sup> )
1	52	Lignite	370	56
2	51.8	Lignite	405	62
3	50.4	Lignite	430	64.7
4	41	High vol. bituminous	503	72
5	40.1	High vol. bituminous	525	113
6	38.5	Bituminous	475	79.2
7	38.4	Bituminous	525	79
8	37	Bituminous	515	86.1
9	34.2	Bituminous	485	107
10	33.5	Bituminous	540	81
11	31.7	Bituminous	560	96.3
12	27.9	Bituminous	560	114
13	19.9	Low vol. bituminous	570	99
14	12.2	Anthracitic	540	124
15	10.0	Anthracitic	625	108
16	9.2	Pet. coke	570	104
17	7.8	Pet. coke anthracite	650	176
18	6.3	Anthracite	650	135
19	6.0	Anthracite	620	147
20	5.5	Anthracite	660	153
21	3.3	Anthracite	675	130
22	1.0	Charcoal	700	190

<sup>a</sup> daf = dried ash free.

the low temperature oxidation of coal [49]. Infrared spectroscopy was used to measure structural changes at the coal surface due to low temperature oxidation. Van der Plaats et al. [49] stated that when coal is heated in an oxygen atmosphere at temperatures above 300°C, combustion processes begin. A DSC curve of this process reveals two exothermic peaks. The first is associated with the formation of quinone-like structures at the surface of the coal, the second with the combustion of the total coal skeleton [26]. The formation of these quinone-like structures proceeds with the uptake of several per cent of oxygen. This exothermic consumption proceeds at low temperatures and can lead to spontaneous heating or pyrophoric reactions. Due to this low temperature oxidation, the utilization properties of the coal may be degraded considerably, i.e., its heat content, which may change by several per cent.

Thermogravimetry (TG), coupled with gas chromatography (GC) and mass spectrometry (MS) (TG/GC/MS), has been employed recently to study coal [50]. The instrument is designed for multiple use, both TG/MS and TG/GC/MS (see Fig. 20). This instrument design also allows for direct mass spectrometry of the TG effluent using the TG/MS mode. In this mode

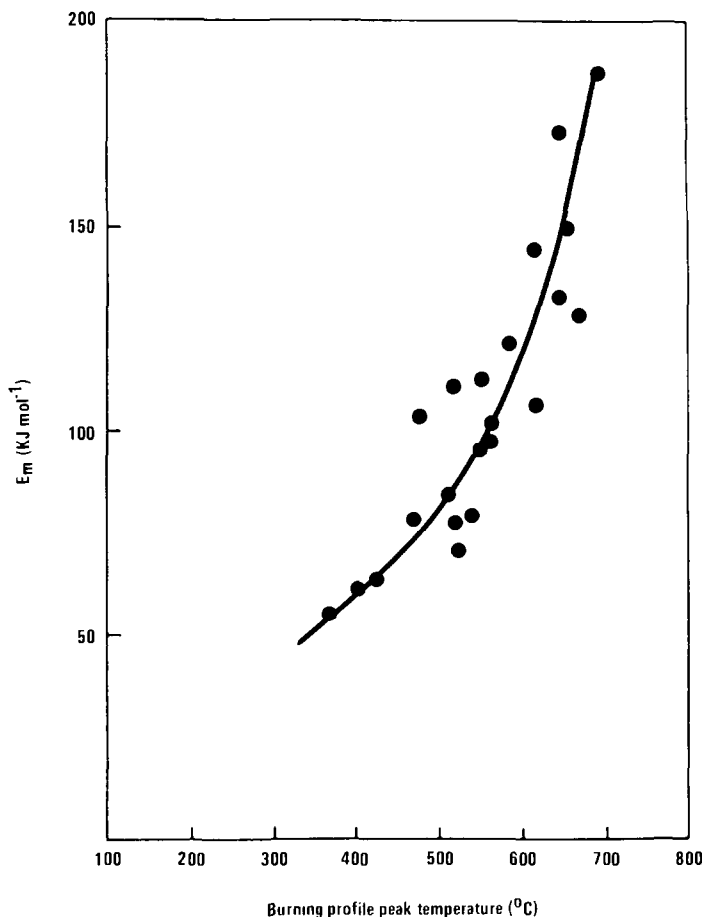


Fig. 19.  $E_m$  versus burning profile peak temperature for 22 solid fuels. (From Cummings [46], p. 1439).

the GC column is inoperative, but the GC oven is heated to 250 or 300°C to prevent condensation in the transfer line.

Figure 21 illustrates a TG curve of the first 3% weight loss from a Pittsburgh coal. The effluent gases were analyzed by MS, the results of which can be seen in Fig. 22. The complexity of the spectrum indicates that several different volatile species form during low temperature pyrolysis of this coal.

To identify these species, the TG/GS/MS mode was employed to analyze the effluent gases during the 0.0–1.6% weight loss. The results can be seen in Fig. 23. These peaks are tentatively identified in Table 3. The chromatogram shows that there are a great number of compounds that are evolved and/or pyrolyzed from this coal under the conditions of this experiment. Some of the materials observed are simply trapped in the coal, whereas others might

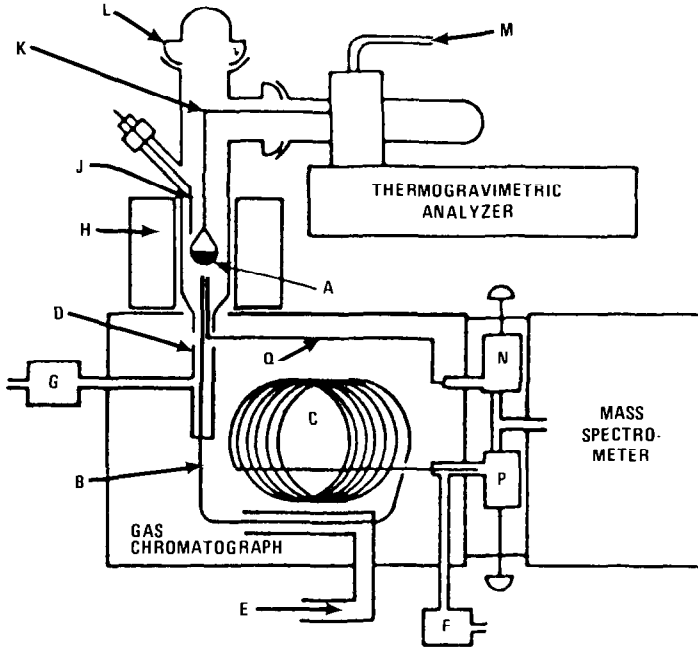


Fig. 20. Design of TG/MS and TG/GC/MS instrumentation. Components are identified as follows: (A) platinum sample pan, (B) front end of fused silica capillary GC column, (C) fused silica capillary GC column, (D) 1/16 in. od glass-lined stainless steel tee, (E) liquid nitrogen-cooled cryogenic trap using 1/8 in od Teflon tubing, (F) flow controller adjusted to deliver  $25 \text{ cm}^3 \text{ min}^{-1}$  helium makeup gas to the jet separator, (G) flow controller adjusted to deliver approximately  $10 \text{ cm}^3 \text{ min}^{-1}$  helium carrier gas to the inlet of the capillary column, (H) TGA furnace, (J) sample thermocouple, (K) balance arm with platinum hang-down wire, (L) 35/25 ground glass joint used as sample loading port, (M) TGA purge gas inlet, (N) needle valve used for TG/MS operation, (P) needle valve used for TG/GC/MS operation, (Q) 1/6 in. od glass-lined stainless steel tubing for TG/MS. (From Whiting and Langvardt [50], p. 1756).

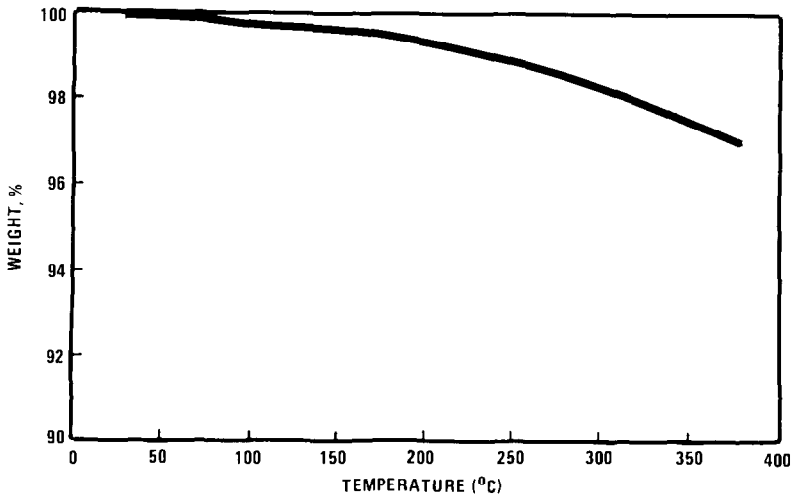


Fig. 21. TG trace of a Pittsburgh bituminous coal. (From Whiting and Langvardt [50], p. 1756).

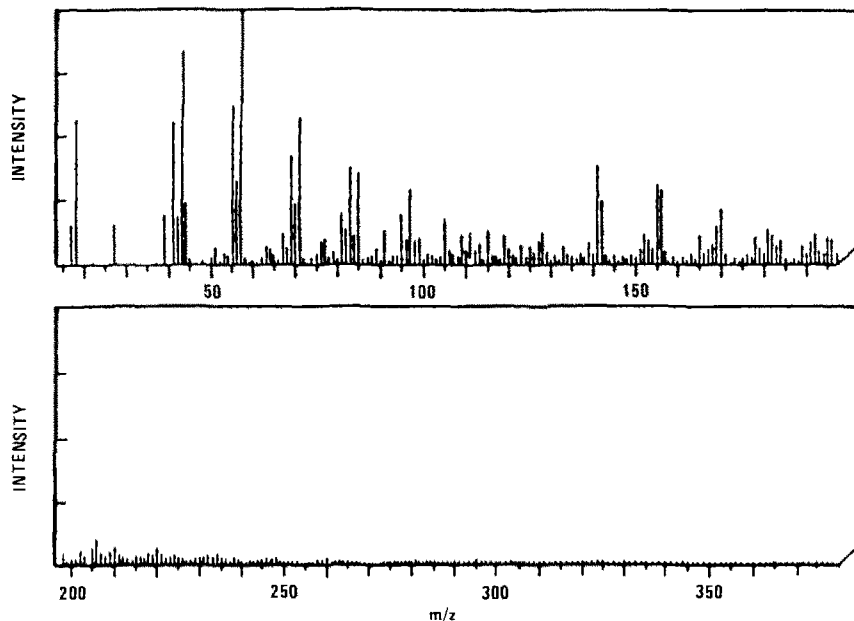


Fig. 22. Mass spectrum acquired at 260°C during TG/MS of a Pittsburgh coal. (From Whiting and Langvardt [50], p. 1756).

result from covalent bond cleavage of complex organic structures found in the coal. The species with the largest peaks in the chromatogram are: carbon dioxide, methylcyclohexane, xylenes, naphthalene, methylnaphthalenes, 1,5-

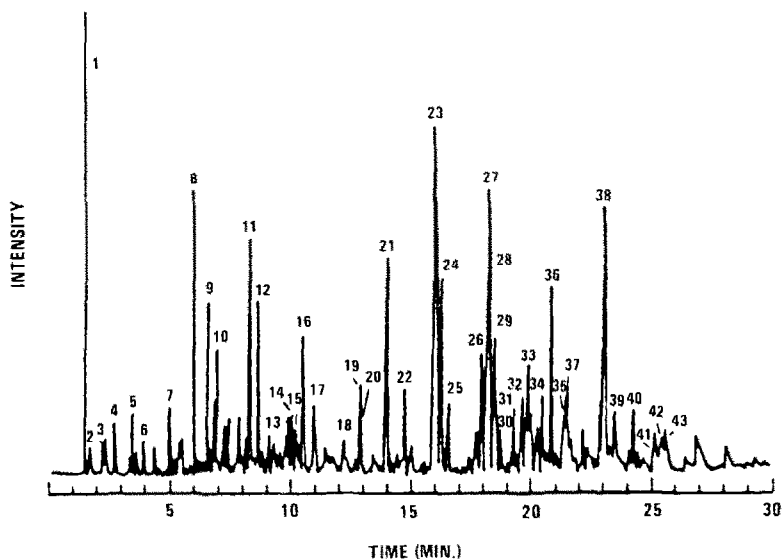


Fig. 23. Reconstructed total ion current gas chromatogram from TG/GS/MS of coal, 0–1.6% weight loss. (From Whiting and Langvardt [50], p. 1757).

TABLE 3

Tentative assignment of gas chromatographic peaks from the TG/GC/MS experiment on coal sample, 0–1.6% weight loss

*1	carbon dioxide	*23	methylnaphthalene
2	sulfur dioxide	*24	methylnaphthalene
3	methylbutane	25	<i>n</i> -tridecane or a methyldecane
4	methylene chloride	26	2,6- or 2,7-dimethylnaphthalene
5	2-methylpentane	*27	1,5- or 1,6-dimethylnaphthalene
6	<i>n</i> -hexane	28	<i>n</i> -tetradecane
7	cyclohexane	29	2,3-dimethylnaphthalene
*8	methylcyclohexane	30	1,2-dimethylnaphthalene
9	toluene	31	C <sub>14</sub> -alkane
10	2-methylheptane	32	C <sub>3</sub> alkylated naphthalene
*11	xylene isomer	33	pentadecane
*12	xylene isomer	*34	trimethylnaphthalene(s)
13	methylethylbenzene	*35	trimethylnaphthalene(s)
14	trimethylbenzene	36	hexadecane
15	methylethylbenzene	37	phenylbenzaldehyde or methyl dibenzofuran
16	1,3,5-trimethylbenzene	*38	> C <sub>16</sub> branched alkane
17	<i>n</i> -decane	39	anthracene or phenanthrene
18	dimethylethylbenzene	40	alkane
19	<i>n</i> -undecane	41	methylanthracene or methylphenanthrene
20	tetramethylbenzene	42	methylanthracene or methylphenanthrene
*21	naphthalene	43	alkane
22	<i>n</i> -dodecane		

\* Species with largest peaks in the chromatogram.

or 1,6-dimethylnaphthalenes, trimethylnaphthalenes and a long-chain alkane. These are noted in Table 3 by an asterisk.

An analysis of the evolved gases associated with the weight loss of the coal sample between 1.6 and 3.0% resulted in the chromatographic separation shown in Fig. 24. Table 4 lists the peaks identified in Fig. 24. These data show that the dominant species of the evolved gases, those marked by

TABLE 4

Tentative assignment of gas chromatographic peaks from TG/GC/MS experiment on coal sample, 1.6–3.0% weight loss

*1	carbon dioxide	8	alkane
*2	sulfur dioxide	9	alkane
3	methylcyclohexane	10	trimethylnaphthalene
4	alkane	11	alkane
5	alkane and dimethylnaphthalene	*12	≥ C <sub>12</sub> alkane
6	dimethylnaphthalene	13	alkane
7	alkane and dimethylnaphthalene	14	alkane

\* Dominant species.

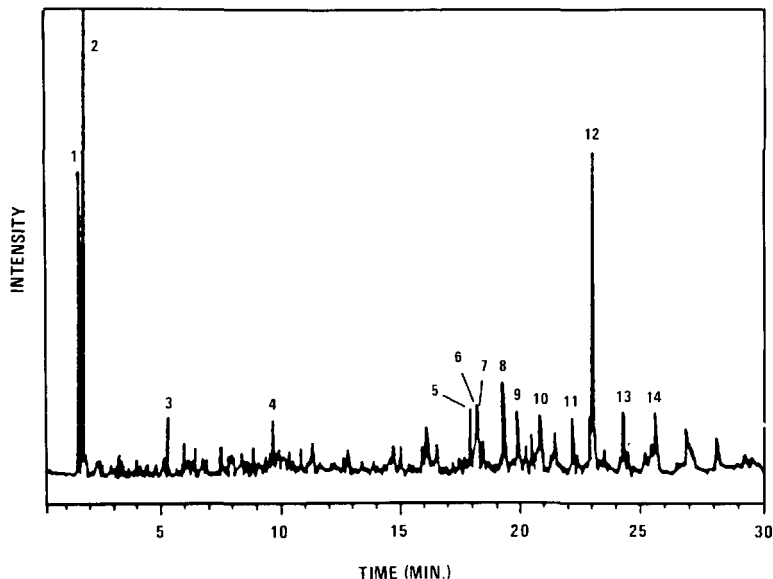


Fig. 24. Reconstructed total ion current gas chromatogram from TG/GS/MS analyses of coal, 1.6–3.0% weight loss. (From Whiting and Langvardt [50], p. 1757).

an asterisk in Table 4, are sulfur dioxide, carbon dioxide and a long-chain alkane. This method of analysis is relatively simple and is a highly efficient approach to evolved gas analysis. It is capable of trapping, separating and identifying compounds ranging from  $\text{SO}_2$  to high alkanes and aromatics.

#### CONCLUDING REMARKS

The above material was assembled to indicate which TA techniques have been applied to characterize the quality of coal for industrial use. Two parameters, atmosphere and heating rate, appear to be the most important variables in the thermal analysis of coals. Controversy and conflict over the validity of some TA techniques still remain. But this is normal, for new methods and new concepts always stimulate different schools of thought. One paramount problem, however, needs to be resolved. Until the problem of exothermicity versus endothermicity of coal in DTA and DSC is resolved, the routine use of these TA methods to glean structural data on coal will be, at best, limited. Over the last eight years the literature search undertaken by the reviewer indicates that investigators have neglected to resolve this problem. Very few research articles were wholly dedicated to the direct solution of this problem.

Research workers, however, are making remarkable progress in coupling other analytical methods with conventional TA methods to help unravel the

scientific mysteries of coal. These other techniques include mass spectroscopy (MS), gas chromatography (GC), infrared spectroscopy (IR) and pulse laser technology. The reviewer, in part, selected the references herewith presented because they illustrate the excellent data that can be gleaned from tandem systems.

More research is needed in coal reactivity (kinetics) to enhance our understanding of the conversion of coal into a cleaner fuel. In addition it would be interesting to explore the use of thermomechanical (TMA) methods to improve the characterization of the caking and agglutinating, swelling, and plasticity properties of coal. This approach could be one of the most rewarding uses of TA methods in coal research in the near future. Both conventional and tandem thermal analysis systems are important for probing and characterizing this heterogeneous, complex and enigmatic material called coal.

## REFERENCES

- 1 M.K. Hubbert, Nuclear energy and the fossil fuels: drilling and production practice, Am. Petrol. Inst., 1956.
- 2 M.K. Hubbert and D.H. Root, in S.P. Parker (Ed.), Outlook for Fuel Reserves, McGraw-Hill Encyclopedia of Energy, 2nd edn., McGraw-Hill, New York, Vol. 19, p. 45.
- 3 M.K. Hubbert, Energy resources: a report to the committee on natural resources, National Academy of Sciences, National Research Council, Publ. 1000-0, Washington, DC, 1962.
- 4 M.K. Hubbert, 1967, Am. Assoc. Petrol. Geol. Bull., 51 (1967) 2207.
- 5 M.K. Hubbert, Energy resources, in Resources and Man, Committee on Resources and Man, National Academy of Sciences, National Research Council, W.H. Freeman, San Francisco, 1969, pp. 157-242.
- 6 P. Averitt, U.S. Geol. Surv. Bull., 1275 (1969).
- 7 C.B. Hatfield, in G. Gallup (Ed.), America Wants to Know: The Issues and the Answers of the Eighties, A. & W. Publishers, Inc., New York, 1983, pp. 407-409.
- 8 K. Rajeshwar, Thermochim. Acta, 63 (1983) 97.
- 9 P.D. Garn, Thermoanalytical Methods of Investigation, Academic Press, New York, 1965.
- 10 R.C. MacKenzie (Ed.), Differential Thermal Analysis V, I and II, Academic Press, London, 1970.
- 11 W.W. Wendlandt, Thermal Methods of Analysis, 2nd edn., Wiley Interscience, New York, 1974.
- 12 C.J. Keatch and D. Dollimore, An Introduction to Thermogravimetry, Heyden, London, 1975.
- 13 M.I. Pope and M.D. Judd, Differential Thermal Analysis, Heyden, London, 1977.
- 14 S.C. Mraw and B.G. Silbernagel, in B.R. Cooper and L. Petrakis (Eds.), Chemistry and Physics of Coal Utilization, American Institute of Physics, New York, 1981, p. 332.
- 15 J.W. Smith, in H. Wiedemann (Ed.), Thermal Analysis, Proc. Third ICTA, Davos, Vol. 3, Birkhauser-Verlag, Basel, 1972, p. 605.
- 16 G.J. Lawson, in R.C. MacKenzie (Ed.), Differential Thermal Analysis, Vol. 1, Academic Press, London, 1972, pp. 705-725.
- 17 R.L. Fyans, Thermal Analysis Applications, Study No. 21, Perkin-Elmer Corporation, Norwalk, CT, 1977.

- 18 R.J. Rosenvold, J.B. Dubow and K. Rajeshwar, *Thermochim. Acta*, 53 (1982) 321.
- 19 M. Offway, *Fuel*, 61 (1982) 713.
- 20 J.W. Cumming and J. McLaughlin, *Thermochim. Acta*, 57 (1982) 253.
- 21 P. Bauer, *Power*, 127 (1983) 91.
- 22 J.P. Elder, *Fuel*, 62 (1983) 580.
- 23 D.M. Aylmer and M.W. Rowe, *Thermochim. Acta*, 78 (1984) 81.
- 24 M.W. Rowe and M. Hyman, *J. Coal Qual.*, 4 (1985) 57.
- 25 H.D. Glass, *Econ. Geol.*, 49 (1954) 294; *Fuel*, 34 (1955) 253.
- 26 D.W. van Krevelen, *Coal*, Elsevier, Amsterdam, 1961, pp. 280–281.
- 27 W.L. Whitehead and I.A. Breger, *Science*, 111 (1950) 279.
- 28 I.A. Breger and W.L. Whitehead, *Conf. Origin, Const. of Coal*, Crystal Cliffs, Nova Scotia, p. 120; *Fuel*, 30 (1951) 247.
- 29 W.L. Whitehead, *Conf. Origin Const. of Coal*, Crystal Cliffs, Nova Scotia, p. 100.
- 30 L.H. King and W.L. Whitehead, *Econ. Geol.*, 50 (1955) 22.
- 31 L.H. King and D.G. Kelley, *Econ. Geol.*, 50 (1955) 832.
- 32 C. Kroger and A. Pohl, *Brennst.-Chem.*, 38 (1957) 179.
- 33 A.F. Boyer and D. Dayen, 3rd Int. Conf. on Coal Science, Valkenburg, 1959.
- 34 A.F. Gaines and R.G. Partington, *Fuel*, 39 (1960) 193.
- 35 O.P. Mahajan, A. Tomita and D.L. Walker Jr., *Fuel*, 55 (1976) 63.
- 36 J.P. Elder and M.B. Harris, *Fuel*, 63 (1984) 262.
- 37 S.St.J. Warne, in C. Karr Jr. (Ed.), *Analytical Methods for Coal and Coal Products*, Vol. III, Academic Press, New York, 1979, pp. 447–477.
- 38 C.M. Earnest, *Thermal Analysis of Clays, Minerals and Coal*, Perkin-Elmer Corporation, Norwalk, CT, 1984, 78 pp.
- 39 S.St.J. Warne, *Thermochim. Acta*, 75 (1984) 138.
- 40 C.M. Earnest, *Thermochim. Acta*, 75 (1984) 219.
- 41 D.W. van Krevelen, F.J. Huntjens and H.N.M. Dormans, *Proc. 1st Int. Congr. Coal Petrology*, Heerlen, 1958 (1960) p. 113.
- 42 C. Kroger, Fr. Kuthe and H. Gondermann, *Brennst.-Chem.*, 38 (1957) 775.
- 43 D.W. van Krevelen, H.A.G. Chermin, H.N.M. Dormans and F.J. Huntjens, *Brennst.-Chem.*, 39 (1958) 77S.
- 44 E.I. Vargha-Butler, M.R. Soulard, H.A. Hamza and A.W. Newmann, *Fuel*, 61 (1982) 437.
- 45 M.A. Seragelden and Wei-Ping Pan, *Thermochim. Acta*, 71 (1983) 1.
- 46 J.W. Cummings, *Fuel*, 63 (1984) 1436.
- 47 M.A. Serageldin and W.-P. Pan, *Thermochim. Acta*, 76 (1984) 145.
- 48 A. De Koranyi and S.G. Williams, *Thermochim. Acta*, 82 (1984) 103.
- 49 G. van der Plaats, H. Soons and H.A.G. Chermin, *Thermochim. Acta*, 82 (1984) 131.
- 50 L.F. Whiting and P.W. Langvardt, *Anal. Chem.*, 56 (1984) 1755.